

# Concentration-induced ferromagnetic-antiferromagnetic phase transition in $\text{Co}_{1-x}(\text{FeMn})_x$

V. P. Antropov, Yu. A. Dorofeev, V. A. Kazantsev, A. Z. Men'shikov, and A. E. Teplykh

*Institute of Metal Physics, Ural Science Center, USSR Academy of Sciences*

(Submitted 25 May 1987)

*Zh. Eksp. Teor. Fiz.* **94**, 216–225 (February 1988)

Using magnetic and electromagnetic methods, we have studied the alloys  $\text{Co}_{1-x}(\text{FeMn})_x$  in the region of the phase transition from long-range ferromagnetic order to antiferromagnetic order. For the first time, we have established that a concentration-induced phase transition takes place in these alloys by way of a spin glass which is found to coexist with ferromagnetic and antiferromagnetic clusters near the corresponding regions of long-range magnetic order. We have assumed a model of the concentration-induced ferromagnet-spin glass-antiferromagnet phase transition which is based on the existence of tricritical behavior on both the ferromagnetic and antiferromagnetic sides. This leads to the formation of regions consisting of a mixture of the two phases (FM + PM) and (AFM + PM), which makes a transition to a cluster spin-glass state at a temperature  $T_f$ .

In studying the concentration-induced ferromagnetic-antiferromagnetic phase transitions which occur in alloy systems with competing exchange interactions, the fundamental question is: what is the ground magnetic state of these alloys in the transition region? It has been shown in a number of articles<sup>1-3</sup> that in magnetic systems which possess disordered sites with FCC lattice symmetry this transition comes about by way of the spin-glass state. Fe-Ni alloys with additions of manganese<sup>2</sup> or chromium<sup>3</sup> constitute examples of such transitions.

However, our recent investigations of Co-Mn alloys,<sup>4</sup> which also have disordered magnetic sites with FCC symmetry, lead us to the conclusion that in these alloys the disruption of long range ferromagnetic order takes place through a region of "frozen-in" superparamagnetic and superantiferromagnetic clusters with sizes  $\sim 100 \text{ \AA}$ , consequently, the FCC symmetry of the lattice, which allows the maximum number of frustrated bonds,<sup>5</sup> and the fulfillment of the condition<sup>6</sup>  $\bar{J}_0 \approx \Delta J$  between the magnitude of the average exchange integral ( $\bar{J}_0$ ) and its fluctuation ( $\Delta J$ ), are not important in the formation of the spin glass state during the transition. As was shown in Ref. 7, the ratio between the magnitude of the ferromagnetic ( $I$ ) and antiferromagnetic ( $K$ ) coupling constants is also important. In the case of the spin glass, the ratio  $K/I$  must be  $\approx 1$ .

Because FeMn and CoMn alloys differ from one another both in the quality and the character of the exchange interaction between unlike ions ( $J_{\text{FeNi}} > 0$ ,  $J_{\text{CoMn}} < 0$ ), it is natural to assume that by introducing iron atoms into the CoMn alloy we increase the ferromagnetic exchange interaction constant due to  $J_{\text{CoFe}}$ ; hence, formation of the spin-glass state in the alloys  $\text{Co}_{1-x}(\text{FeMn})_x$  will be more probable than in the alloys  $\text{Co}_{1-x}\text{Mn}_x$ , where according to our picture,  $K/I \gg 1$  holds. In order to verify this assumption, we decided to replace half the manganese atoms with iron atoms at a given concentration of cobalt, and track the character of the concentration-induced phase transition in the resulting  $\text{Co}_{1-x}\text{Mn}_x$  alloys. In a previous paper<sup>8</sup> we obtained the concentration dependences of the Curie and Néel points in this system; however, the region of the transition from long-range ferromagnetic order to antiferromagnetic order re-

mained unstudied, and a full magnetic phase transition diagram was not constructed.

## EXPERIMENTAL METHOD

For investigative purposes, we smelted alloys of quasi-binary composition described by the formula  $\text{Co}_{1-x}\text{Mn}_x$  from pure components in which the content of iron and manganese were kept in identical proportions, while  $x$  took on the following values: 0.2, 0.3, 0.34, 0.40, 0.42, 0.44, 0.46, 0.50, 0.54, 0.56, 0.58, 0.60, 0.64, 0.70, 0.80. The metals were melted in a pure argon atmosphere. The alloy ingots were hammered into 8–10 mm diameter rods, which then underwent a homogenizing anneal in a helium atmosphere for 100 hours at 1300 K. For the magnetic measurements we used samples which were 6 mm in diameter and 1 mm thick. Cylindrical samples with 6 mm diameter and 50 mm length were used for coherent and incoherent neutron scattering. These samples were also used to study the susceptibilities in AC fields.

The magnetic measurements were carried out using a vibromagnetometer in the temperature interval 4.2–800 K in magnetic fields up to  $1.6 \times 10^6 \text{ A/m}$ . The sample temperature was measured using a copper-iron-copper thermocouple with an accuracy of  $\pm 1 \text{ K}$ . The relative measurement errors of the magnetization came to 1.5–2%.

The neutron-diffraction investigations were carried out on a diffractometer ( $\lambda = 1.81 \text{ \AA}$ ) set up at one of the horizontal channels of the IVV-2M reactor. As a monochromator we used a strained single crystal of germanium in the (111) plane. The measurements were made in a helium cryostat over the temperature interval 4.2–400 K both at large angles for determination of long-range magnetic order and at small angles (the minimum  $q = 0.09 \text{ \AA}^{-1}$ ) for separating out the incoherent neutron scattering by magnetic inhomogeneities.

## EXPERIMENTAL RESULTS

In order to identify the basic magnetic states of the alloys under study, we first measured the magnetization curves at 4.2 K, some of which are shown in Fig. 1. The cooling from room temperature down to 4.2 K was carried

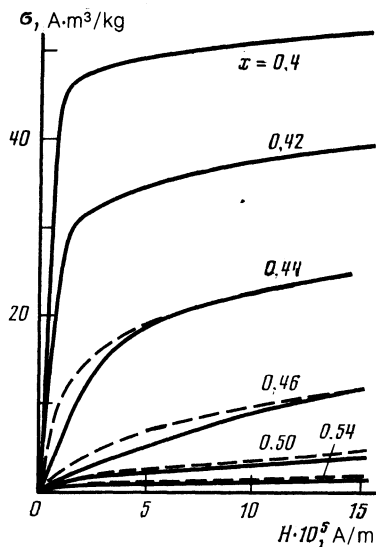


FIG. 1. Magnetization curves for  $\text{Co}_{1-x}(\text{FeMn})_x$  alloys of different compositions at 4.2 K. Continuous curves—samples cooled to 4.2 K in the absence of a magnetic field ( $\sigma_{ZFC}$ ), broken curves—samples cooled in a magnetic field of prescribed value ( $\sigma_{FC}$ ).

out at a rate of 1 K/sec at a given value of  $H$ ; every 10 seconds a sample was taken out and its magnetization measured. It was established that all alloys with  $x \geq 0.4$  have dependences  $\sigma(H)$  which exhibit saturation in fields  $1-2 \times 10^5$  A/m, which are characteristic of ferromagnets. In this case, the functions  $\sigma(T)$  measured at small fields ( $0.05 \times 10^5$  A/m) exhibited sharp kinks in the magnetization at the Curie temperature<sup>9</sup>; these kinks allowed us to determine the values of the Curie points, which showed good agreement with those given in Ref. 8 for those alloys with  $x \leq 0.4$ .

For the alloys with  $x \geq 0.4$ , the magnetization curves had different characteristics. For these alloys the curves show more resemblance to Langevin curves, which are characteristic for superparamagnets. Here we still observed a difference in the shape of the  $\sigma(H)$  curves obtained on samples which were first cooled to 4.2 K without a magnetic field (ZFC) compared to curves for samples in the corresponding measurement field (FC). Measurement of  $\sigma_{ZFC}(T)$  for fixed values of the external field  $H$  were carried out in the following fashion: a sample was cooled in the absence of a field down to 4.2 K at a rate of 1 K/sec. The field was switched on; the sample was then removed and heated over a period of 100 sec at a rate of 0.1 K/sec, and the running value of magnetization was recorded. Then, without switching off the field, the curve  $\sigma_{FC}(H)$  was recorded at the same rates of cooling and heating.

As is clear from Fig. 1, in the region of fields where it was determined  $\sigma_{FC}$  is larger than  $\sigma_{ZFC}$ . As the temperature is increased from its value for a cooled sample, the difference between  $\sigma_{ZFC}(H)$  and  $\sigma_{FC}(H)$  disappears; this is shown in Fig. 2 for the  $x = 0.44$  alloy. Consequently, the region of compositions  $0.4 \leq x \leq 0.54$  is characterized by the phenomena of magnetic viscosity and irreversibility of the curves  $\sigma_{ZFC}(H)$  and  $\sigma_{FC}(H)$ , which is characteristic of the spin-glass type of magnetic system. In order to establish the type of magnetic state and to determine the temperature of the phase transition, the temperature dependences of the rever-

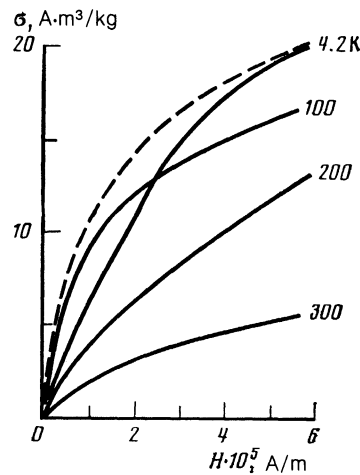


FIG. 2. Magnetization curves for  $\text{Co}_{1-x}(\text{FeMn})_x$  alloys with  $x = 0.46$  after cooling the alloy to the labeled temperatures in zero magnetic field (continuous curves) and in a magnetic field of prescribed value (broken curves).

sible ( $\chi_{FC}$ ) and irreversible ( $\chi_{ZFC}$ ) susceptibilities were measured. The results of these measurements are shown in Figs. 3, 4 for the three alloys with  $x = 0.46, 0.50, \text{ and } 0.54$ . It is clear that the temperatures  $T_i(H)$  at which the susceptibilities  $\chi_{FC}$  and  $\chi_{ZFC}$  begin to disagree depend strongly on the value of the measurement field. In this case, as is clear from Fig. 3, for the alloys adjacent to the ferromagnetic region there exists a certain critical field ( $H_0$ ) below which the beginning of the disagreement lies at a higher temperature than the maximum in the irreversible susceptibility. This implies that there is a ferromagnetic component in the system with an anisotropy field of  $\sim 1$  kOe. When this field is exceeded, we observe a characteristic shift in  $T_i(H)$  toward the low-temperature side. For the alloys with  $x = 0.50$ , however, this phenomenon of irreversibility begins at the maximum of  $\chi_{ZFC}(T)$  in the minimum measured field, which argues in favor of a spin-glass state in this alloy (Fig. 4a).

A somewhat different type of irreversibility is observed for the alloy with  $x = 0.54$ , which adjoins the antiferromagnetic region of composition. Here, in contrast to the  $x = 0.50$  alloy, the temperature for which the disagreement between

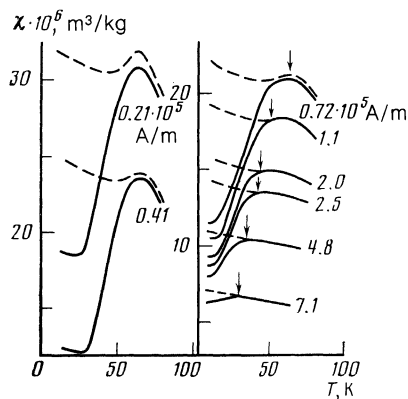


FIG. 3. Temperature dependence of  $\chi_{ZFC}$  (continuous curves) and  $\chi_{FC}$  (broken curves) at the labeled magnetic fields for the  $x = 0.46$  alloy.

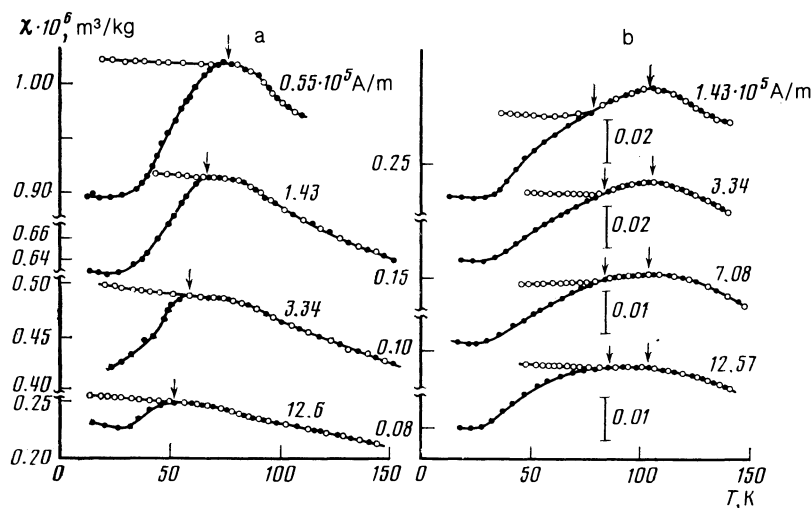


FIG. 4. Temperature dependence of  $\chi_{ZFC}$  (filled circles) and  $\chi_{FC}$  (open circles) obtained at the labeled magnetic fields for the  $x = 0.5$  alloy (a) and the  $x = 0.54$  alloy (b).

$\chi_{FC}$  and  $\chi_{ZFC}$  begins increases with increasing field, and for a certain field  $H \approx 12$  kOe  $T_i(H)$  coincides with the temperature maximum of the irreversible susceptibility.

In the presence of this complex behavior of the magnetic system as a function of the magnitude of the external field, it is natural that a question should arise as to the procedure used to determine the transition temperature  $T_f(0)$  in the degenerate spin-glass state. There exist various approaches to defining this temperature.<sup>10</sup> In our opinion, the most physically justifiable definition of  $T_f(0)$  is the temperature maximum of the real part of the dynamic susceptibility (the AC susceptibility), which is obtained at zero magnetic field by extrapolating its frequency dependence  $T(0, \nu)$  to  $\nu = 0$ . A second method consists of measuring the field dependence of the temperature maximum of the irreversible susceptibility at constant current, and extrapolating its value to  $H = 0$ . With little error (i.e., too small to notice in constructing the phase diagram), we can use the maximum in the curve  $\chi_{ZFC}(T)$  as  $T_f(0)$  when the latter is measured in a weak magnetic field, and have done so for this paper.

In order to observe long-range antiferromagnetic order, we carefully measured the intensity of inelastic neutron scattering in the neighborhood of the (110) reflection at liquid helium temperatures. In Fig. 5a we present portions of the intensity difference ( $J_{4.2K} - J_{300K}$ ) in the neutron diffraction patterns for certain alloys located at the boundary where antiferromagnetism of the  $\gamma$ -FeMn type appears. It is clear that for alloys with  $x \geq 0.60$  this reflection has a width at half maximum which is instrument-limited, while the temperature dependence of its intensity allows us to establish the Néel point for these alloys (Fig. 5b). For the alloys with  $0.50 < x < 0.60$ , we observed a broadened maximum in the intensity difference near the (110) reflection which is evidence for the presence of antiferromagnetic clusters with sizes on the order of  $\sim (100-150)$  Å. The Néel temperature for these clusters cannot be accurately identified by using these neutron diffraction patterns, because of the low reflection intensity; however, it approximately corresponds to the temperature maximum of the low-frequency susceptibility. As for the transition to a system of superantiferromagnetic clusters in a spin-glass state, this transition was observed by using the above-mentioned field dependence of the temperature  $T_i(H)$  at which the system passes into the nonergodic

state. On the basis of an extrapolation of this temperature to  $H = 0$ , we also estimated the phase transition point for the degenerate spin-glass state.

From these magnetic and neutron-diffraction studies we constructed a magnetic phase diagram of the alloys  $\text{Co}_{1-x}(\text{FeMn})_x$ , which is illustrated in Fig. 6. On it we note the regions of ferromagnetic and antiferromagnetic long-range order, and also the transition region between them.

## DISCUSSION OF EXPERIMENTAL RESULTS

### A. Exchange interaction between iron atoms and atoms of manganese and cobalt

So as to decide on the character of the exchange interaction between iron atoms and atoms of manganese and cobalt, we carried out a theoretical investigation of the electronic structure of pure cobalt, and also cobalt with manganese and iron impurities. We used the  $T$ -matrix formalism, which is directly related to the Green's function; this latter function contains all the information about the electronic structure of

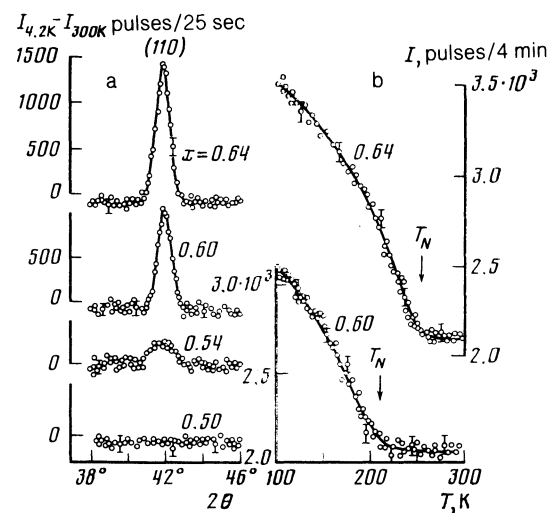


FIG. 5. Portions of the neutron diffraction diagrams for alloys (a) near the (110) reflection and (b) the temperature dependence of the latter, for certain  $\text{Co}_{1-x}(\text{FeMn})_x$  alloys.

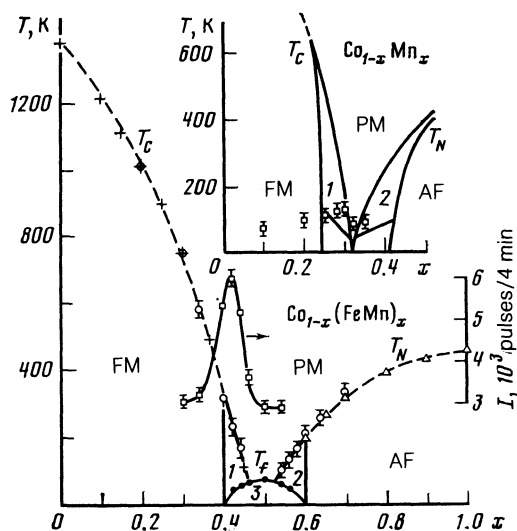


FIG. 6. Magnetic phase diagram of  $\text{Co}_{1-x}(\text{FeMn})_x$  alloys. The Curie temperature ( $T_C$ ), the Néel temperature ( $T_N$ ), and the alloy temperature  $T_f$ : +,  $\Delta$  (Ref. 8); O,  $\bullet$ —data from the present paper. FM—ferromagnetic, AF—antiferromagnetic, PM—paramagnetic; 1—FM + PM, 2—AF + PM, 3—spin glass. In the inset we show the magnetic phase diagram of  $\text{Co}_{1-x}\text{Mn}_x$  alloys from Ref. 4. Here we also present the results ( $\square$ ) of the concentration-induced dependence of the small-angle neutron scattering for  $q = 0.1 \text{ \AA}^{-1}$ ,  $q = 4\pi \sin(\theta/\lambda)$ .

the crystal. A more detailed description of this method can be found in Ref. 11.

The results of self-consistent computer calculations of the densities of states for “up” and “down” spins leads to the conclusion that cobalt in its FCC and HCP modifications is ferromagnetic, with a value of its magnetic moment equal to  $1.7 \mu_B$ . In order to determine the stability of ferromagnetic or antiferromagnetic configurations of impurity atoms of manganese or iron in cobalt, we calculated the change in the crystal energy connected with replacing a cobalt atom by an impurity atom. The calculation was carried out using the following equation from Ref. 12:

$$\delta E = \frac{1}{\Pi} \text{Im Sp} \int_0^{\varepsilon_F} d\varepsilon \{ \ln[1 - (P_{\uparrow}^0 - P_{\uparrow})T_{\uparrow}^0] + \ln[1 - (P_{\downarrow}^0 - P_{\downarrow})T_{\downarrow}^0] \}, \quad (1)$$

where  $\varepsilon_F$  is the Fermi energy,  $P_{\uparrow}^0$  and  $P_{\downarrow}$  are potential parameters and  $T_{\uparrow}^0$  is the scattering matrix. From these calculations we found that for impurity atoms of iron in the FCC and HCP modifications of cobalt the ferromagnetic configuration is the most stable, with values of the magnetic moment equal to 2.37 and  $2.38 \mu_B$ , respectively; these moments coincide reasonably well with the experimental data on the saturation magnetization.<sup>13</sup>

An entirely different situation is predicted for manganese impurities in cobalt. In both modifications, the manganese can be situated both ferromagnetically and antiferromagnetically. However, whereas in the HCP modification the changes in crystal energy due to introduction of the impurity manganese atom are roughly the same (0.55 and 0.5 eV), in the FCC modification the energy change is smaller

for the antiferromagnetic position (0.11 eV) than for the ferromagnetic position (0.28 eV). From the results of these calculations it therefore follows that the exchange interaction between atoms of cobalt and iron is ferromagnetic, while that between cobalt and manganese is antiferromagnetic; we should assume that this is also the case in both the corresponding binary alloys and the ternary alloy  $\text{Co}_{1-x}(\text{FeMn})_x$ .

## B. Comparison of the magnetic phase diagrams

Let us discuss the phase diagrams for the alloys  $\text{Co}_{1-x}(\text{FeMn})_x$  and  $\text{Co}_{1-x}\text{Mn}_x$ , taking into account the character of the exchange interaction between the atoms (Fig. 6). The important feature which distinguishes these diagrams is the absence of a region of composition corresponding to the degenerate spin-glass state in  $\text{Co}_{1-x}\text{Mn}_x$  alloys, and the presence of such a region for  $\text{Co}_{1-x}(\text{FeMn})_x$ . In this latter case, the replacement of half the atoms of manganese by iron atoms causes a rather strong shift in the transition concentration region from 0.25–0.4 to 0.4–0.6.

The cause of this behavior is doubtless connected with the ratio of exchange interaction constants for the two systems. We may assume that because  $J_{\text{CoMn}} < 0$  and  $J_{\text{MnMn}} < 0$ , the antiferromagnetic exchange interaction coupling constant ( $K = 1/2|J_{\text{CoMn}} + J_{\text{MnMn}}|$ ) is considerably larger than the ferromagnetic constant ( $I = J_{\text{CoCo}}$ ) in CoMn alloys, i.e.,  $K/I \gg 1$ . At the same time, the inclusion of a strong ferromagnetic interaction in the  $\text{Co}_{1-x}(\text{FeMn})_x$  alloys apparently makes this ratio closer to unity; consequently, the region of critical concentration for these alloys, in contrast to  $\text{Co}_{1-x}\text{Mn}_x$  alloys, lies near  $x = 0.5$ .

Using this picture, we can also explain the character of the reconstruction of the ferromagnetic state into the antiferromagnetic state as the concentration of the components changes. It is clear that because of the strong antiferromagnetic interaction in  $\text{Co}_{1-x}\text{Mn}_x$  alloys, in order to disrupt a topologically infinite ferromagnetic cluster we require a smaller number of frustrated bonds than in the  $\text{Co}_{1-x}(\text{FeMn})_x$  alloys. Besides, the blocks into which the infinite ferromagnetic cluster collapses have larger dimensions in the  $\text{Co}_{1-x}\text{Mn}_x$  alloys than in the  $\text{Co}_{1-x}(\text{FeMn})_x$  alloys. Experimental proof of this assertion is found from the absence of small-angle neutron scattering for momentum transfers of  $q \approx 0.1 \text{ \AA}^{-1}$  in  $\text{Co}_{1-x}\text{Mn}_x$  alloys and its appearance in  $\text{Co}_{1-x}(\text{FeMn})_x$  (Fig. 6). It is well-known that such scattering arises from magnetic inhomogeneities of dimensions 10–20  $\text{\AA}$  (Ref. 14); its absence is evidence of the presence of inhomogeneities whose scale is significantly larger—so large that the scattering should be detectable only for  $q \leq 0.01 \text{ \AA}^{-1}$ .

## C. A model of the concentration-induced ferromagnetic-antiferromagnetic phase transition

Let us discuss the region of composition  $0.40 \leq x \leq 0.60$ , where the replacement of ferromagnetic long-range order by antiferromagnetic order takes place, in more detail. In Fig. 6 we have enclosed this region within the two tricritical points. The existence of tricritical behavior in the magnetic system of the  $\text{Co}_{1-x}(\text{FeMn})_x$  alloys near the ferromagnetic and antiferromagnetic regions is confirmed first of all by the

form of the magnetization curves, which are close to Langevin-like (Fig. 1), and secondly by the presence of a broad halo in the neighborhood of the antiferromagnetic (110) reflection (Fig. 5a). The small-angle neutron scattering also points to strongly inhomogeneous magnetic structure in the neighborhood of the ferromagnetic tricritical point which lies in this range of compositions (Fig. 6), as does the irreversible behavior in  $\sigma_{ZFC}$  and  $\sigma_{FC}$  versus temperature near  $T_c$ . The tricritical behavior from the ferromagnetic and antiferromagnetic sides attests to the presence in these systems of two non-interacting order parameters. Actually, we can write down the thermodynamic potential for a system with two coupled order parameters in the form

$$\Phi = \Phi_0 + \frac{1}{2}A_1 \mathbf{m}^2 + \frac{1}{4}C_1 \mathbf{m}^4 + \frac{1}{2}A_2 \mathbf{l}^2 + \frac{1}{4}C_2 \mathbf{l}^2 + \lambda \mathbf{m}^2 \mathbf{l}^2, \quad (2)$$

where  $\mathbf{m} = \mathbf{M}_1 + \mathbf{M}_2$  and  $\mathbf{l} = \mathbf{M}_1 - \mathbf{M}_2$  are respectively the ferromagnetic and antiferromagnetic order parameters, while  $\mathbf{M}_1$  and  $\mathbf{M}_2$  are the magnetizations of the sublattices; when the interaction constant between them satisfies  $\lambda = 0$ , the potential splits into two independent parts, each of which gives rise to the presence of a tricritical point for  $C_1 < 0$  ( $C_2 < 0$ ).<sup>15</sup> In the  $T - x$  plane, the second-order phase transition line becomes two first-order transition lines at these points; between these first-order lines, there is a mixture of the ferromagnetic and paramagnetic phases on one side while on the other the mixture is antiferromagnetic plus paramagnetic. The physical reason for this magnetic subdivision in the system is the accumulation of frustrated bonds as the alloy approaches the critical concentration. In our case the addition to the ferromagnet of the antiferromagnetically-interacting pairs Mn-Mn and Mn-Co leads to destruction of the ferromagnetic long-range order within several coordination spheres of a frustrated bond. In the bulk, such fluctuations can isolate components of the magnetic moment perpendicular to the direction of the spontaneous magnetization, which implies that another order parameter will appear in the system. The transition to the paramagnetic state in such magnetically inhomogeneous regions (or, according to Saslov and Parker,<sup>16</sup> "melting" of the frustration sites) will take place at a lower temperature than the Curie temperature for a topologically infinite ferromagnetic cluster. Therefore, above  $T_f(0)$  we can assume that between the two first-order phase transition lines there exists a mixture of paramagnetic and ferromagnetic clusters with a range of effective sizes. Among these clusters we may also find some, both ferromagnetic and paramagnetic, which are topologically infinite.

Analogous arguments can be advanced for the antiferromagnetic alloy side. Lowering the temperature leads to various magnetic ground states for such alloys. If the ferromagnetic or antiferromagnetic correlations (clusters) are large enough (i.e., the inverse correlation lengths satisfy  $K < 0.01 \text{ \AA}^{-1}$ ), then the system of clusters at the point  $T_f(0)$  can undergo the usual Néel subdivision with the absence of any indication of a cooperative phase transition. This case apparently is realized in  $\text{Co}_{1-x}\text{Mn}_x$  alloys. If the inverse correlation length satisfies  $K > 0.01 \text{ \AA}^{-1}$ , then the most likely occurrence is a cooperative phase transition at  $T_f(0)$  to a cluster spin-glass state. Because of the random anisotropy, the clusters form their own subsystem of disordered frozen-in macroscopic spins within the spin-glass matrix; these macroscopic spins interact among themselves through the

layer between them of misoriented spins which make up the spin-glass phase. The resulting state will be strongly degenerate in energy, and can with equal validity be called a degenerate spin-glass state.<sup>17</sup>

Apparently this last case is precisely the one which is encountered in the  $\text{Co}_{1-x}(\text{FeMn})_x$  alloys under discussion here. In fact, the  $H-T$  diagrams shown in Fig. 7 for the alloys with  $x = 0.46$  and  $0.5$  also suggest this. When we construct plots on log-log scales of functions such as  $\tau = 1 - T_i(H)/T_f(0) = (H/H_a)^\gamma$  ( $H_a$  is the field anisotropy) for each alloy, we can distinguish two linear portions having different slopes, and consequently different exponents  $\gamma$ . The theoretical values  $\gamma = 2$  for the Heisenberg model<sup>18</sup> and  $\gamma = 0.66$  for the Ising model<sup>19</sup> are not observed in the present case. For alloys with  $x = 0.46$ , the exponent  $\gamma = 0.77$  in the small field region when  $T_i(H)$  reduces to  $T_f(0)$ , and  $\gamma = 0.36$  for high fields. For the alloy with  $x = 0.50$ , we have  $\gamma = 1.0$  and  $0.5$  for the same field ranges. Consequently, we see here evidence of at least two subsystems, having different dependences of the freezing-in temperature on field as a consequence of the different values of effective anisotropy constant. The first of these is a system of large particles with small anisotropy fields which depend more strongly on field; the second is a system of particles which are small in size but which have high anisotropy fields. An estimate of the magnitude of this latter field for the alloy with  $x = 0.46$  gives  $H_a = 45 \text{ kOe}$ , while for the  $x = 0.50$  alloy  $H_a = 55 \text{ kOe}$ . We can assume that the first subsystem, which is characterized by a small anisotropy field, has disordered frozen-in macrospins, while the second subsystem with the large anisotropy field is more homogeneous and closer in its properties to a spin glass in the sense of Edwards and Anderson. However, the dependence of  $T_f$  on field in our case is weaker; this could be connected with the presence of interactions between the two subsystems we have postulated here.

## CONCLUSION

The ferro-antiferromagnetic concentration-induced phase transition in  $\text{Co}_{1-x}(\text{FeMn})_x$  alloys which we have investigated here is relevant to a number of similar transitions which take place by way of a cluster spin-glass state, which in its turn is a result of tricritical behavior of the system from the ferromagnetic and antiferromagnetic sides. This situation apparently is general enough to cover many of these concentration-induced phase transitions; however, be-

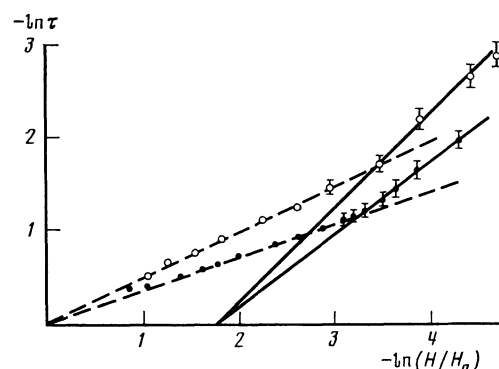


FIG. 7.  $H-T$  diagram for  $\text{Co}_{1-x}(\text{FeMn})_x$  alloys with  $x = 0.46$  (●) and  $x = 0.5$  (○).

cause the sizes of the ferromagnetic and antiferromagnetic inhomogeneities (clusters) can differ, the character of the phase transitions at  $T_f(0)$  can also be different; either the transition takes place cooperatively when the clusters are small ( $< 20 \text{ \AA}$ ), or a Néel subdivision occurs when the clusters are large ( $> 100 \text{ \AA}$ ).

- <sup>1</sup>M. B. Medvedev, *Izv. Vuzov. Fizika (University Physics Bulletin)* **10**, 3 (1984).  
<sup>2</sup>A. Z. Menshikov, P. Burlet, A. Chamberod, and J. L. Tholence, *Solid State Commun.* **39**, 1093 (1981).  
<sup>3</sup>A. Z. Menshikov, G. A. Taksei, and A. E. Teplykh, *Fiz. Met. Metalloved.* **54**, 465 (1982) [*Phys. Met. Metallogr. (USSR)* **54**(3), 41 (1984)].  
<sup>4</sup>A. Z. Menshikov, G. A. Taksei, Yu. A. Dorofeev *et al.*, *Zh. Eksp. Teor. Fiz.* **89**, 1269 (1985) [*Sov. Phys. JETP* **62**, 734 (1985)].  
<sup>5</sup>M. V. Medvedev and M. V. Sadovskiy, *Phys. Stat. Sol.* **B109**, 49 (1982).  
<sup>6</sup>S. Kirkpatrick and D. Sherrington, *Phys. Rev.* **B17**, 4384 (1978).

- <sup>7</sup>G. A. Petrakovski, E. V. Kuz'min, and S. S. Aplesnin, *Fiz. Tverd. Tela (Leningrad)* **24**, 3298 (1982) [*Sov. Phys. Solid State* **24**, 1872 (1982)].  
<sup>8</sup>K. Adachi, K. Sato, M. Matsui, and S. Mitani, *IEEE Trans. Magn.* **8**, 693 (1972)].  
<sup>9</sup>I. K. Kamilov and Kh. K. Aliev, *Usp. Fiz. Nauk* **140**, 639 (1983) [*Sov. Phys. Usp.* **26**, 696 (1983)].  
<sup>10</sup>G. A. Taksei, A. M. Kostyshin, Yu. P. Grebenyuk, and I. I. Sych, *Zh. Eksp. Teor. Fiz.* **90**, 1843 (1986) [*Sov. Phys. JETP* **63**, 1081 (1986)].  
<sup>11</sup>O. Gunnarsen, O. Jepsen, and O. K. Andersen, *Phys. Rev.* **B27**, 7144 (1983).  
<sup>12</sup>B. L. Gyorffy and G. M. Stocks, *Phys. Rev. Lett.* **50**, 374 (1983).  
<sup>13</sup>J. S. Kouvel, *J. Phys. Chem. Soc.* **16**, 107 (1960).  
<sup>14</sup>A. Z. Men'shikov and V. A. Shestakov, *Phys. Met. Metallogr.* **43**, 722 (1977).  
<sup>15</sup>L. D. Landau, *Zh. Eksp. Teor. Fiz.* **7**, 19 (1937).  
<sup>16</sup>G. Saslov and P. Parker, *Phys. Rev. Lett.* **56**, 1074 (1986).  
<sup>17</sup>I. Ya. Korenblit and E. F. Shender, *Zh. Eksp. Teor. Fiz.* **89**, 1785 (1985) [*Sov. Phys. JETP* **62**, 1030 (1985)].  
<sup>18</sup>M. Gabay and G. Toulouse, *Phys. Rev. Lett.* **47**, 201 (1981).  
<sup>19</sup>J. T. L. de Almeida and D. J. Thouless, *J. Phys.* **A11**, 983 (1978).

Translated by Frank J. Crowne